REPÜLÉSTUDOMÁNYI KÖZLEMÉNYEK
On-Line tudományos folyóirat
XXVII. évfolyam 2015. 2. szám

György Bicsák[1] – Árpád Veress[2]

VERIFICATION OF A COST EFFICIENT SOLUTION TO SIMULATE THE AIRFLOW CONDITIONS IN AN OIL-TO-AIR HEAT EXCHANGER OF A SMALL AIRCRAFT APPLYING POROUS MATERIAL[3][4]

The scope of the paper is to introduce a simple, cost-efficient method, which is capable to simulate the air flow of a heat exchanger and can be integrated into more complex simulations. A partner institute provided data about a heat exchanger, which geometry has been replaced by a cuboid with rounded edges and porous domain has been applied into the volume. The cuboid has been extended by 5 times length of the original depth of the porous domain in upstream and downstream directions to form the flow channel, by which two fluid domains have been attached on the porous domain. Tetra elements have been used for the spatial discretization. The physical characteristics of the heat exchanger have been determined from the available data (pressure drop values at different mass flow rates). The parameters of the porous media (K_{loss} and K_{perm}) have been calculated by Darcy's law. The volume porosity has been identified by sensitivity analyses due to missing information. Finally, the available and the numerically calculated pressure drops in the function of the mass flow rates are compared with each other. The differences between the two investigated cases are less than 2.3%, which verifies the expectations.

KÖLTSÉGHATÉKONY MÓDSZER VERIFIKÁCIÓJA EGY KISREPÜLŐGÉP OLAJ-LEVEGŐ HŐCSERÉLŐJÉNEK ÁRAMLÁSTANI SZIMULÁCIÓJÁRA PORÓZUS ANYAG MODELLEZÉSÉNEK FELHASZNÁLÁSÁVAL

A jelen publikáció célja, hogy egy olyan egyszerű és költséghatékony módszert mutasson be, mely alkalmas egy hőcserélőben áramló levegő modellezésére, ugyanakkor integrálható egy nagyobb, komplexebb szimulációba. Az együttműködő partner intézmény által biztosított adatok szolgáltak alapul a vizsgálathoz. A hőcserélő geometriáját egy téglatesttel modelleztük, amelyben egy porózus anyagban áramló közeget definiáltunk. A tartomány előtt és után a porózus térfogat ötszörös vastagságának megfelelő rá-, és leáramlási teret hoztunk létre. Tetraéder típusú elemeket alkalmaztunk a térbeli háló elkészítésére. A gyártó által biztosított adatok (adott tömegáramhoz tartozó nyomásesés) alapján meghatároztuk a hőcserélő karakterisztikáját és Darcy egyenletének felhasználásával a porózus közeg tulajdonságai (K_{loss} és K_{perm}). A térfogati porozitást érzékenységi vizsgálatok segítségével állítottuk elő több szimuláció lefuttatását követően. A mérési és a numerikus áramlástani szimulációk eredményeinek összehasonlítása 2.3%-os eltérést mutattak egymáshoz képest, ami elfogadható a számítás hitelességének tekintetében.

INTRODUCTION

As the aviation safety increases continuously, according to its highly cost efficient solutions, the usage demand of the air transport systems is also expanding. Naturally, the mainstream and determining developments and researches are concentrated at the large aircraft manufacturer

[1] Assistant Lecturer, BME Department of Aeronautics, Naval Architecture and Railway Vehicles, gybicsak@vrht.bme.hu
[2] Associate Professor, BME Department of Aeronautics, Naval Architecture and Railway Vehicles, averess@vrht.bme.hu
[3] Reviewed: László Kavas (PhD), Assistant Lecturer, National University of Public Service Department of Military Aviation, kavas.laszlo@uni-nke.hu
[4] Reviewed: Béla Varga(PhD), Assistant Lecturer, National University of Public Service Department of Military Aviation, bela.varga@uni-nke.hu

companies, like Airbus or Boeing, but because of the new trends, and the growing traffic in the personal flight systems, the role of smaller aircraft manufacturer companies also increases [28]. Furthermore the propagation of different Unmanned Aeronautical Vehicles (UAV) [10] also demands some cheaper but still accurate calculation and design methods.

Recently, one of the most dynamically improving research field is the Computational Fluid Dynamics (CFD), which is a good alternative of the highly cost and time demanding experimental test measurements in wind tunnels or laboratories. Due to the excellent features of wide range of visualization – even by using virtual reality –, easy and fast regeneration, reproducibility, high level parameterization, field and geometric model independence together with coupling more physics and optimization, the simulation methods often are not just a more cost efficient solution than experimental measurements, but even provide more details and information about a given problem.

Although the Large Eddy Simulation (LES) or Direct Numerical Simulation (DNS) can provide higher resolution level of the turbulence fluctuations of the flow, which is simulated, because of their computational performance demands for complex simulations the Reynolds Averaged Navier-Stokes (RANS) simulations are still preferable. This is even more true for smaller aircraft manufacturer companies, where the necessary computational requirements (as computers and work hours) are not always available, in their case the simpler solutions are more rewarding, if the accuracy is satisfying.

These solutions make possible for smaller companies to be involved more in research and development processes. The ESPOSA Project (Efficient Systems and Propulsion for Small Aircraft) targets these smaller companies, and tries to provide them development tools and technologies.

The ESPOSA Project

The 7th Framework Programme, International ESPOSA Project began in 2011. The 3 year long project aims to develop and integrate novel manufacturing and design technologies and methods for small gas turbines, in the range of approx. 160 kW up to 1000 kW, instead of piston engines. According to the development of the small gas turbines' control schemes and monitoring opportunities, their efficiency is also more exploitable [28][30] The project also deals with engine related systems, such as fuel and electronic systems, structural elements, fire protection system, control and monitoring, etc., in order to achieve better efficiency, safety and pilot workload reduction. [47] According to the expectations, the new engine systems and engine technologies gained from ESPOSA should reduce the direct operational costs (DOC) with 10-14%, furthermore they will significantly reduce the pilot workload. "The ESPOSA project is oriented on turbine engine technologies tailored for a small aircraft up to 19 seats (under CS-23/FAR23) operated on the scheduled and non-scheduled flights. The research work comprises performance improvements of key engine components, their improved manufacture in terms of costs and quality." [47]

During the project, four different small, propeller driven aircraft configurations have been considered; 2 pusher and 2 tractor configurations. The colleagues of BME Department of Aero-

nautics, Naval Architecture and Railway Vehicles participate in several industrial and international research projects. One of them is the ESPOSA program, in which the task of the Department is to improve design specifications of the engine intake channel, nacelle and an oil-to-air heat exchanger of a newly developed turboprop aircraft by means of CFD.

The scope of the paper

The above mentioned oil-to-air, plate-fin type heat exchanger has to be taken into consider in the later simulations. Thus the behaviour of the heat exchanger and its effect to the external airflow have been investigated.

Researching the related literature, it is clear, that the heat exchangers have got wide range of applications and functions. The main scope of designing a heat exchanger is to reduce or increase a fluid temperature with a different temperature levelled fluid flow [14][41]. The efficiency of the heat exchangers are determined by numerous parameters, like the shape [39], flow conditions [56], control method [52] the airflow turbulence, which can be regulated by vortex generators [13][39][56]. They can be operated individually or in networks [3]. Besides the most common applications, like lubrication oil cooling, fuel warming etc. there are special applications also, for example for cryogenic purposes [35]. They can apply supercritical [42] or nanofluids [4], and also fundamentally new solutions and materials are also experimented, like foams [19][31], where sometimes the basic calculation methods have to be developed, and new perspectives have to be implemented, like the genetic algorithm [50].

Their characteristics can be investigated from different viewpoints, but the most important parameters are the heat transfer and the caused pressure drop. The former one was investigated by Fernández-Sear, Diz, and Uhía [26], a comparison was made experimentally between spiral fin-and-tube heat exchangers by Pongsoi, Pikulkajorn, and Wongwises [43]. In order to determine the proper heat transfer of different heat exchangers, CFD simulations have been performed by Cheng, Tsai, Cheng, and Chen [12]; Taler and Ocłoń [16][18]; Yang and Li [54]; Kumar, Gangaschrayulu, Rao and Barve [52]; and by Čarija, Franković, Perčić and Čavrak [60]. The generated pressure drop is also a determining problem, according to its effect on other units (like pumps, pipes), which are connected to the investigated heat exchanger [25]. The pressure drop can be calculated analytically, as it was described by Parikshit, Spandana, Krishna, Seetharam, and Seetharamu [10], it can be measured experimentally, like it was publicated by Yin, Bullard, and Hrnjak [27], or by using CFD methods, like Saad, Clément, Fourmigué, Gentric and Leclerc have published it [46]. Besides the CFD methods the Finite Element Method (FEM) analysis is also a solution to determine the heat transfer [19]. Both parameters were investigated experimentally by Kearny and Jacobi [49].

In the possession of the detailed characteristics of a heat exchanger, its behaviour can be predicted, and also this knowledge makes possible the optimization methods, for minimizing for example the pressure drop [36][53], or the specific entropy generation rate [55]; or determining of further, special parameters like the Colburn factor and Fanning factor [37].

In our investigation the goal is different. The characteristics of the heat exchanger was determined, we had to examine the external airflow around the rotors and engine nacelle, furthermore inside the air intake duct. The heat transfer between the hot lubrication oil and cooling ram air is

indifferent from our viewpoint. Basically the heat exchanger had to be taken into consider as a component which wades the air, flow through it, resulting in pressure drop effect. Additionally this pressure drop had to be simulated with the lowest possible computational requirement, so a detailed internal flow simulation is not practical according to the necessity of the fine mesh. In order to satisfy these demands, the whole heat exchanger has been replaced by a porous domain.

The porous medium theoretically consists skeletal portion of the material, often called matrix, and the pores are filled with fluid [9]. It can be characterized by its porosity, permeability, tensile strength, electrical conductivity [33]. It can be used in wide range of applied science and engineering, like filtration, soil mechanics, geomechanics, petroleum engineering, bio-remediation, hydrogeology, biophysics, material science etc. [4] The usability of the porous material is represented by the following publications: an oil spill application presented by Adebajo, Frost, Kloprogge, Carmody, and Kokot [40]; application in Stirling regenerators published by Tew, Simon, Gedeon, Ibrahim, and Rong [44]; Berg has investigated the charging process of a stratified thermal storage tank [1]; or Neale, Derome, Blocken and Carmeliet have simulated the vapor flow between porous material to represent a building [2], and similar problem has been handled by Steeman, Janssens, and Paepe [23]. The behavior, heat transfer capability and flow conditions of different porous media have been characterized by Nield and Bejan [15]; Krishnakumar and Nair [32]; Nebbali and Bousri [45]; Menon and Kumar [2]; and Sharafat, Mills, Youchison, Nygren, Williams, and Ghoniem [49].

This paper introduces a unique, different method; however porous material usage in heat exchanger has been published by Delavar and Azimi [34], for our application no similar article has been published. Our scope is to simulate the external air flow around an engine nacelle, which is influenced by an air-to-air plate-fin type heat exchanger, but the minimum possible computational requirement and neglecting the heat transfer inside the heat exchanger.

THEORETICAL FUNDAMENTALS

Around the investigated engine nacelle, and inside the heat exchanger it is reasonable to assume that the airflow is incompressible, hence the incompressible Navier-Stokes equations are suitable to describe the phenomenon. In general, the Coriolis term can be neglected, as its effects is minimal.

The simulation of turbulent airflows are usually complex, because of the presence of the turbulent, continuously fluctuating characteristics phenomenon, which produce a wide range of time and length scales. For example the turbulent scales are varying between 10 m to 0.01 mm. Based on this effect, LES or DNS simulations are not the best choice to handle this engineering application, because of the computational time and requirement demand. The Reynolds number, which defines the ration of inertial forces to viscous forces, highly influences the range of scales. To consider the effect of unresolved small scales on the behaviour of large scales turbulence models have to be applied. Since the turbulence models can’t manage both the boundary layers on the walls and the turbulent structures in the wake, so well considered (experimental-based) simplifications are also necessary.

Governing Equations

The basic governing equations for a RANS simulation are well-known, thus in this paper they are only shortly overviewed, and not detailed here. The used Ansys CFX software solves the set of unsteady form of the Navier-Stokes equations in their conservation form. The set of equations contain the continuity, momentum, and total energy equations, completed by the incompressible, ideal, real gas and liquid equation of state (the supplemental terms are not stated here).

The continuation equation is discussed in the following form: [7]

$$\frac{\partial \rho}{\partial t} + \nabla \cdot (\rho U) = 0 \tag{1}$$

where ρ is the density, and U is vector of velocity ($U_{x,y,z}$). The momentum equations: [7]

$$\begin{gathered} \frac{\partial (\rho U)}{\partial t} + \nabla \cdot (\rho U \otimes U) = -\nabla p + \nabla \cdot \tau + S_M \\ \text{where } \tau = \mu \left(\nabla U + (\nabla U)^T - \frac{2}{3} \delta \nabla \cdot U \right) \end{gathered} \tag{2}$$

In the equation p is the pressure, τ is the shear stress tensor and S_M is momentum source. In the description of the shear stress tensor, μ is the dynamic viscosity and δ is the Kronecker Delta function. The total energy equation can be written in the following form: [7]

$$\begin{gathered} \frac{\partial (\rho h_{tot})}{\partial t} - \frac{\partial p}{\partial t} + \nabla \cdot (\rho U h_{tot}) = \nabla \cdot (\lambda \nabla T) + \nabla \cdot (U \cdot \tau) + U \cdot S_M + S_E \\ \text{where } h_{tot} = h + \frac{1}{2} U^2 \end{gathered} \tag{3}$$

In this equation h_{tot} represents the specific total enthalpy, S_E is energy source, h is the enthalpy (internal energy of the fluid), and λ is thermal conductivity.

Porous Domain

In Ansys CFX the flow in porous media can be simulated by using either of two models: [7]

- using a fluid domain together with a momentum loss model. In this case the porosity is accounted for only through this loss term, other terms in the governing equations are not changed. Sometimes this formulation is called “superficial velocity formulation”.
- using a domain that involves one or more fluids and an optional solid. All the terms in the governing equations are modified by the porosity, as well as the loss term. This model can be called the “true velocity formulation”, or the “full porous model”.

However we are looking for a simple solution, in order the get more accurate results, the full porous model was used during the simulation, thus its equations are described here.

The full porous model is based on the commonly used Darcy’s law for pressure drop determination, and on the generalization of the Navier-Stokes equations. It is usually applied where the geometry is too complex to resolve with a mesh. The model can be used to simulate flows in rod or tube bundles, or between fins, where such effects are important, because both advection and diffusion terms are retained by the model. During the derivation of the continuum equa-

tions, the infinitesimal control volumes and surfaces are assumed relatively large to the interstitial spacing of the porous medium, but on the other hand they're small to the applied scales that are wanted to be resolved. Because of this consideration the control cells and control surfaces are assumed to contain both solid and fluid regions. [7]

One of the key parameters of the whole investigation is the volume porosity (γ), which shows the ration of the available volume (V') in an infinitesimal control cell surrounding the point, and the physical volume of the cell (V) in the following form: [7]

$$\gamma = \frac{V'}{V} \tag{4}$$

In a porous medium the general scalar advection-diffusion equation can be written in the following form: [7]

$$\frac{\partial}{\partial t}(\gamma\delta\phi) + \nabla\cdot(\rho\boldsymbol{K}\cdot\boldsymbol{U}\phi) - \nabla\cdot(\Gamma\boldsymbol{K}\cdot\nabla\phi) = \gamma S \tag{5}$$

where ϕ is an additional variable (non-reacting scalar), $\boldsymbol{K}$ is a symmetric second rank tensor, called the area porosity tensor, $\boldsymbol{U}$ marks the true velocity, Γ is the diffusivity, and S is a source term, which contains transfer terms from the fluid to the solid parts of the porous medium.

Consequently, the mass and momentum conservation equations are:

$$\frac{\partial}{\partial t}\gamma\delta + \nabla\cdot(\rho\boldsymbol{K}\cdot\boldsymbol{U}) = 0 \tag{6}$$

$$\frac{\partial}{\partial t}(\gamma\delta\boldsymbol{U}) + \nabla\cdot(\rho(\boldsymbol{K}\cdot\boldsymbol{U})\otimes\boldsymbol{U}) - \nabla\cdot\left(\mu_e\boldsymbol{K}\cdot\left(\nabla\boldsymbol{U} + (\nabla\boldsymbol{U})^{\boldsymbol{T}} - \frac{2}{3}\delta\nabla\cdot\boldsymbol{U}\right)\right) = \gamma S_M - \gamma\nabla p \tag{7}$$

where μ_e is the effective viscosity, and S_M is a momentum source.

The applied momentum source is implemented into the software as a force per unit volume acting on the fluid. The applied isotropic losses in the porous regions can be formulated by using permeability and loss coefficients in the following directions: [7]

$$S_{M,i} = -\frac{\mu}{K_{perm}}U_i - K_{loss}\frac{\rho}{2}|\boldsymbol{U}|U_i \tag{8}$$

where K_{perm} is the permeability and K_{loss} is a quadratic loss coefficient. The linear component of this source represents viscous losses and the quadratic term represents inertial losses. [7] The (8) can be called also as Darcy's law.

INTRODUCTION OF THE SIMULATION

In order to accurately handle the airflow around the engine nacelle, wing and rotors of the given aircraft configuration, the behaviour of the installed oil cooler heat exchanger had to be investigated. The scope of the department's in the project was to examine the airflow conditions around the engine nacelle, and inside the air inlet duct, and make modification suggestions to improve the aerodynamic characteristics of the configuration. Thus, the heat transfer process is

less interesting from our viewpoint, than the pressure drop inside the heat exchanger's cold side, where the external cooling ram air flows through.

In order to integrate the heat exchanger component to the whole model, in this paper the necessary parameters of the porous material, which replaces the heat exchanger, are calculated and investigated for further researches.

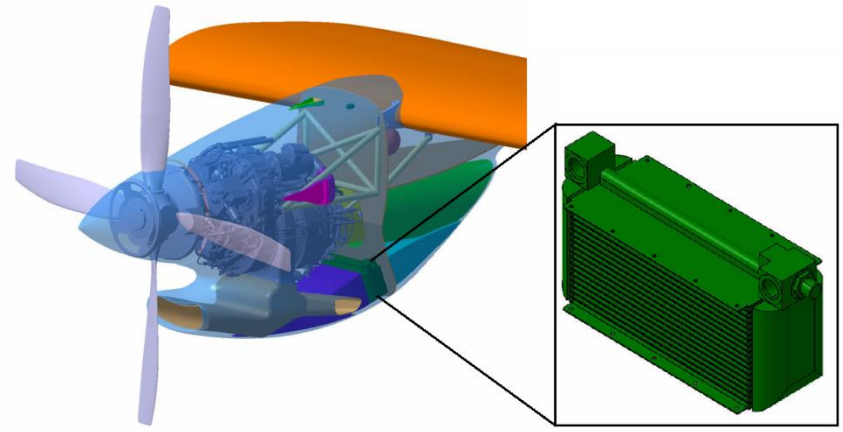

Figure 1. The institute provided detailed original geometry [5]

In order to reduce the computational requirements, only one wing with the related engine nacelle and air ducts have been implemented (see in Figure 1). The high-wing configuration determines the position of the engine and the nacelle below the wing. Downstream of the rotor at the lower section of the nacelle is the air duct inlet. The internal air duct is completed with a particle and ice separator device. The separated particles leave the airflow on the sidewall duct outlets. Upstream of the gas turbine section there is a static vane air intake device, and downstream of the gas turbine the hot exhaust gases can leave the engine through the exhaust pipe. At the bottom of the nacelle takes place the cross-flow, oil-to-air type heat exchanger, which cools down the engine oil, which uses ambient ram airflow. The air enters the heat exchanger through a NACA air intake and leaves it through the heat exchanger outlet, right below the exhaust pipe.

From this configuration the illustrated (Figure 1) heat exchanger is investigated. Based on the partner institute (EVEKTOR) provided data, the heat exchanger's main dimensions: [20]

- Core (WxHxD) 6.26" High x 12.99" Wide x 4.72" Deep
- Cold Side Fin: 0.250" Louvered Fin 11 FPI
- Hot Side Fin: 060" Lance and Offset Fin 8 FPI

Geometry

The investigated geometry is much simpler than the original one. Because the whole heat exchanger is replaced by a porous material, for the simulation only the bounding volume had been kept, all the internal fins and tubes have been deleted.

[5] ESPOSA Integrated Project – Level 2, Aeronautics and Air Transport; BE2 TR2 WP6.4 Requirements; prepared by EVEKTOR; 1st October 2011, GRANT AGREEMENT NO. ACP1-GA-2011-284859-ESPOSA

The inlet and outlet boundary conditions mustn't be affected by the airflow, thus the heat exchanger inlet and outlet surfaces have been extracted with 600 mm in both directions, and besides the porous domain – aka. heat exchanger – two other fluid domains have been created. The complete geometry of the investigated geometry is illustrated by Figure 2.

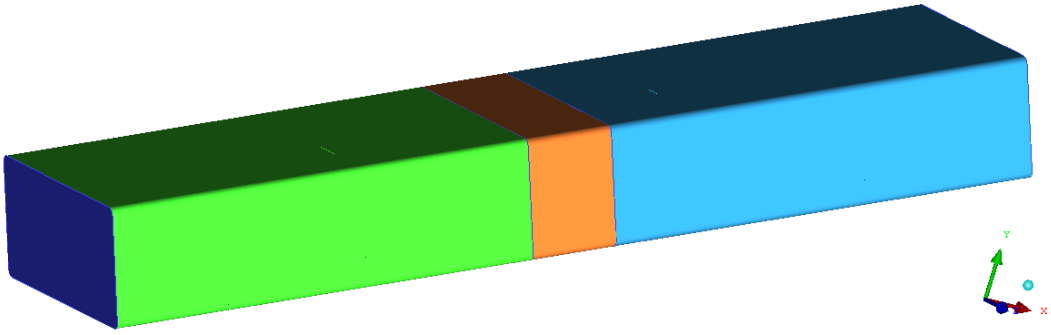

Figure 2. The geometry of the heat exchanger (in the middle with orange colour) completed by two auxiliary fluid domains (green and blue)

Mesh

The advantage of the introduced simplified geometry that the meshing process is not complicated, hence hexa elements could be used. Despite that, tetra elements have been used, because later, at the whole simulation (when the rotors, engine nacelle, wing, and air ducts are also participating in the airflow) the complexity of the geometry requires tetra elements, and in this way the simulation and the porous domain expectedly are going to provide similar results.

Similarly the size of the mesh was fitted to the overall mesh sizes, so every surface and volume elements were set to 10 mm. On the walls boundary layers have been applied; with 8 mm height 8 inflation layers were inserted with 1.5 prism ratio.

In this way totally 1204103 elements and 294923 nodes have been created. The mesh is illustrated by

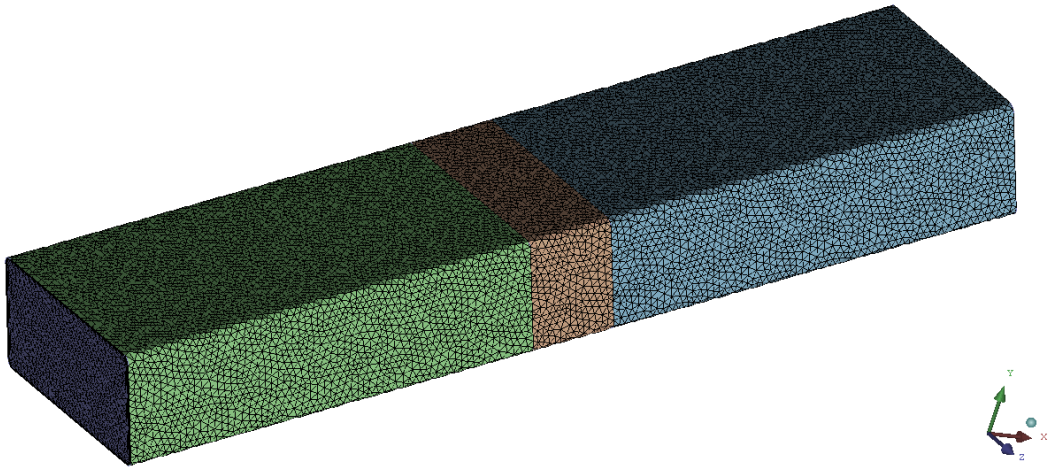

Figure 3. The generated mesh of the investigated geometry

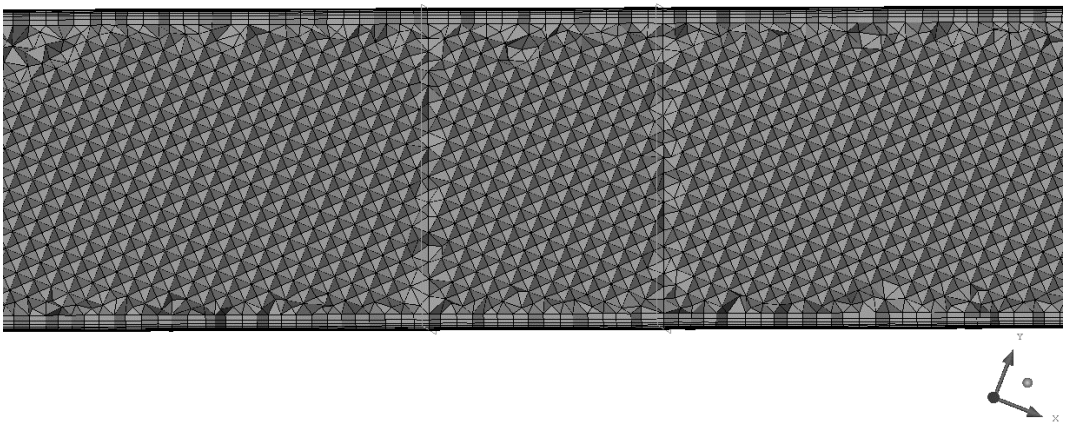

Figure 4. The created inflation layers in the cross section of the model

Boundary Conditions

The heat exchanger was designed to remove 1208 Btu/min. from 90 lbs/min. of SAE 50 oil at 99 °C using 105 lbs/min. of air at 50 °C (see Figure 5). A bypass circuit with a thermostat is included. The construction is a vacuum brazed aluminium core with fabricated or cast tanks. [20]

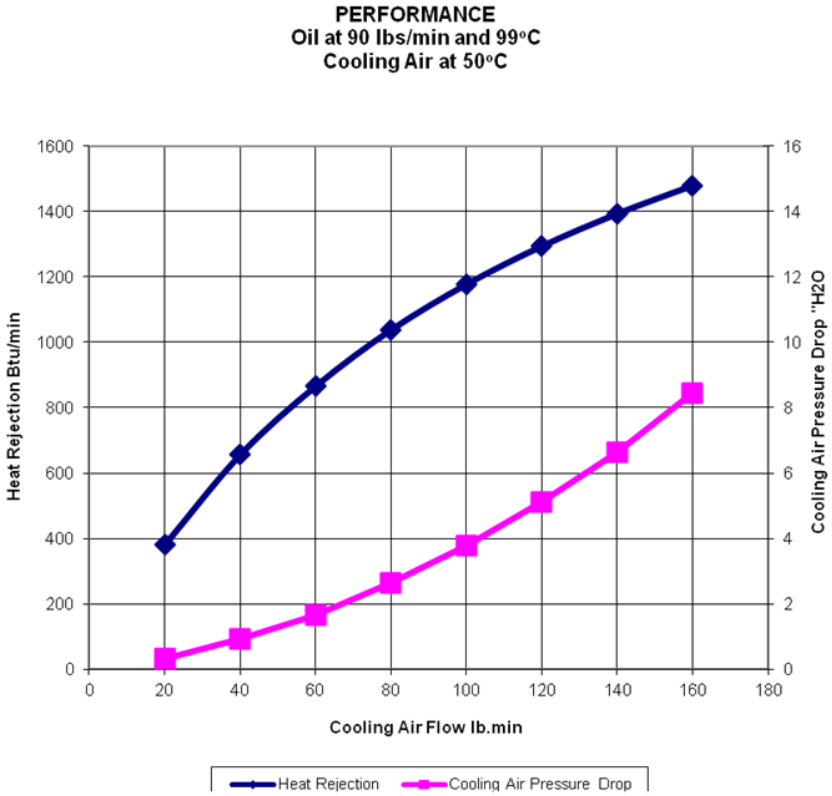

Figure 5. Heat exchanger performance: the heat rejection and cooling air pressure drop in the function of the cooling air flow [6]

[6] ESPOSA Integrated Project – Level 2, Aeronautics and Air Transport; BE2 TR2 WP6.4 Requirements; prepared by EVEKTOR; 1st October 2011, GRANT AGREEMENT NO. ACP1-GA-2011-284859-ESPOSA

	Cold Side	Hot Side
Fluid	Air	Oil
Flow Rate	105 lbs/min.	90 lbs/min.
Temperature In	50ºC(122.0 ºF)	99ºC(210.2 ºF)
Temperature Out	76.5ºC(169.6 ºF)	84.2ºC(183.6 ºF)
Inlet Pressure	7.4"H2O	100 psig
Pressure Drop	4.0 in. H_2O	24.6 psig
Passes	1	1
Flow Arrangement	Cross Flow	
Calculated Heat Rejection	1208 Btu/min	
Requested Heat Rejection	1240 Btu/min.	
Effectiveness	.54	

Table 1. The main design points of the oil cooler heat exchanger [5]

Based on the given parameters, the necessary parameters had to be calculated manually. At first, the provided data were transformed into SI dimensions. The converted values can be seen in Table 2. The 6th row marks the sampling data, which was detailed in Table 1. These values were the base of the calculations, and later the volume porosity determination process.

Cooling air mass flow [lb/min]	Pressure Drop ["H2O]	Cooling air mass flow [kg/s]	Pressure Drop [Pa]
20	0.4	0.1511975	1195.627
40	1.05	0.3023949	3138.520
60	1.7	0.4535924	5081.414
80	2.6	0.6047898	7771.574
100	3.8	0.7559873	11358.454
105	4	0.7937866	11956.268
120	5.1	0.9071847	15244.241
140	6.6	1.0583822	19727.842
160	8.45	1.2095797	25257.615

Table 2. SI converted heat exchanger characteristics

The reference pressure was set to 101325 Pa (p_0), from which the inlet pressure values ($p_{inlet,i}$) have been calculated, as the following: the pressure difference ($\Delta p_{inlet,6}$) which was given as inlet pressure in Table 1 in the 6th row is a positive pressure difference compared to the environmental (reference) pressure. So this pressure value has been decreased with the pressure drop (11956.268 Pa) in case 6 (105 lb/min mass flow inlet), and the active pressure drop was added to it, because the pressure drop, caused by the heat exchanger fins, decreases the airflow, so at the inlet it appears as a pressure increment. This calculation can be summarized as:

$$p_{inlet,i} = \left(p_0 + \Delta p_{inlet,6} - \Delta p_6\right) + \Delta p_i \quad (9)$$

To determine the required parameters for Darcy's law, the pressure drop values have to be plotted in the function of the air flow velocities. To calculate the velocity, at first the densities have been calculated, as the function of inlet pressure, *R* gas constant for ideal air, and the inlet

temperature (T_0), which was considered to constant 50 °C in every cases. In this way the densities are:

$$\rho_i = \frac{p_{inlet,i}}{RT_0} \tag{10}$$

In this way the velocities are:

$$v_i = \frac{\dot{m}_i}{\rho_i A} \tag{11}$$

where A is the area of the heat exchanger inlet surface (0.054 m^2). The calculated velocities have been confirmed with simulations; in the inlet domains the inlet mass flow has been determined together with the inlet pressure, which was set as an outlet pressure. The calculated and simulated velocities can be compared in Table 3. As it can be seen, the differences were lower than 0.2 m/s in every case.

Cooling air mass flow [kg/s]	Pressure Drop [Pa]	Inlet pressure [Pa]	Inlet relative pressure [Pa]	Density [kg/m^3]	Velocity - analytic [m/s]	Velocity - simulated [m/s]
0.1511975	1195.627	112683.45	11358.45	1.21556	2.303	2.204
0.3023949	3138.520	114626.35	13301.35	1.23652	4.529	4.395
0.4535924	5081.414	116569.24	15244.24	1.25748	6.680	6.528
0.6047898	7771.574	119259.40	17934.40	1.28650	8.706	8.542
0.7559873	11358.454	122846.28	21521.28	1.32519	10.564	10.394
0.7937866	11956.268	123444.10	22119.10	1.33164	11.039	10.866
0.9071847	15244.241	126732.07	25407.07	1.36711	12.289	12.114
1.0583822	19727.842	131215.67	29890.67	1.41547	13.847	13.669
1.2095797	25257.615	136745.44	35420.44	1.47512	15.185	15.007

Table 3. The calculated and simulated parameters for the porous domain

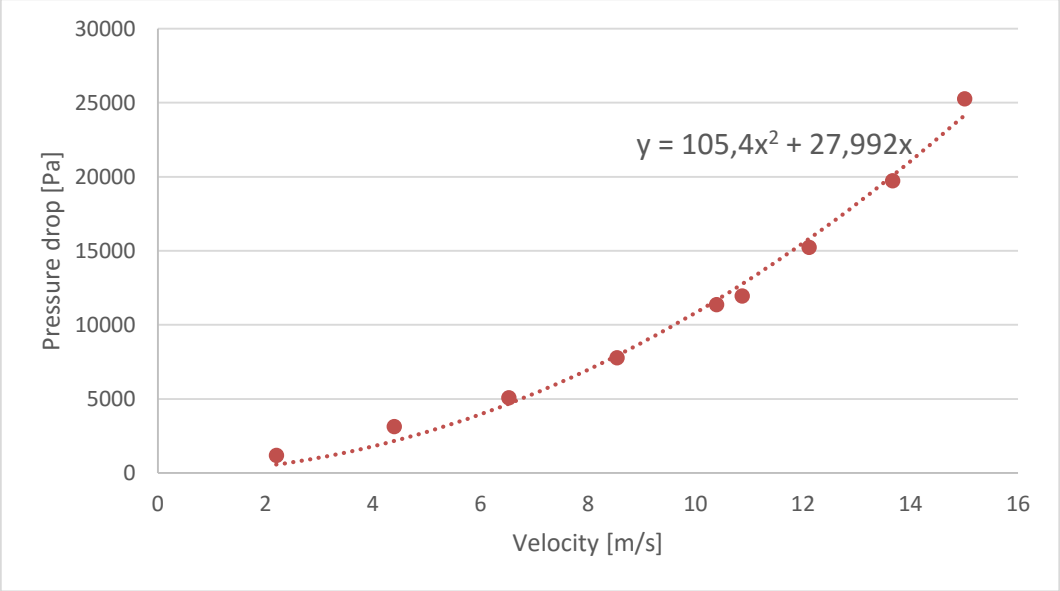

Figure 6. The velocity - pressure drop diagram

The calculated values have been plotted, see Figure 6. A trend curve has been placed into the points. It is important, that Darcy's law requires a parabolic function, which crosses the "y" axis in 0 point. [7] The equation of the polynomial is: $y = 105.4\ x^2 + 27.992\ x$.

If we consider the air's dynamic viscosity to $1.962*10^{-5}$ kg/ms [20], by using equation (8) the K_{loss} and K_{perm} can be calculated: [56]

- K_{loss} = 158.3013814 1/m
- K_{perm} = $7.00915*10^{-07}$ d $1/m^2$

The scope is to determine the volume porosity. To determine this value, the following simulation has been prepared: the introduced three-domain mesh has been divided into three sections: two normal fluid domains with air ideal gas air flow, and in the middle the porous domain (see Figure 7). The already mentioned 6th sample parameters have been applied:

- The domains have been connected to each other with fluid-domain general interface
- In the inlet surface static pressure has been set with 22119.1 Pa relative pressure
- In the outlet surface mass flow outlet have been created with 0.7937866 kg/s
- At the outer wall normal non-slip walls have been set
- The reference pressure was 101325 Pa
- SST turbulence model have been applied
- Total energy heat transfer model has been set, which includes the viscous work term
- Full porous model has been set
- For the porous domain the already introduced K_{loss} and K_{perm} have been set, with 0.5 volume porosity for first try
- Because the model is simple, no long run-time or high iteration number are required, so only 100 iteration steps have been set. The turbulence numeric was set to High Resolution, the residual target was 10^{-5}. All other settings were let in the default option.

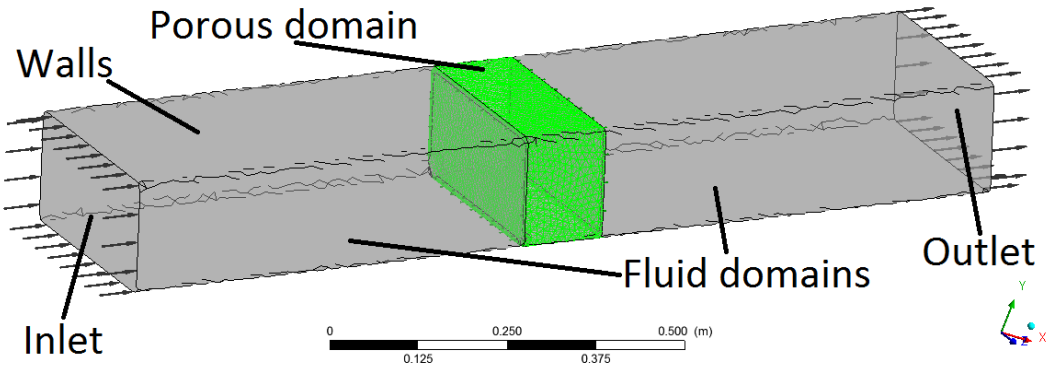

Figure 7. Boundary conditions of the model

Results, Evaluation

As we expected it, because of the simple geometry, the simulations have been converged (the imbalances have reached 0) in average 20-30 iteration steps, so later the target iteration target has been modified to 50 steps. After a simulation, the target parameter was investigated, and the volume porosity has been modified to meet with the demands.

Expectedly, the simulation – the volume porosity – required some "fine tuning". The surface averaged pressure value has been investigated between the porous domain inlet and outlet surfaces, thus the pressure differences were calculated. The target pressure drop was 12287 Pa. The relative errors have been calculated, compared to the target pressure drop value. In this way, the best volume porosity could be determined, as Table 4 shows.

Volume porosity [-]	Pressure difference [Pa]	Relative error [%]
0.3	18910	53.9025
0.35	13587	0.105803
0.358	12950	0.053959
0.36	12798	0.041589
0.363	12573	0.023277
0.381	11358	0.075608
0.4	10707	0.128591
0.7	3543	0.711646

Table 4. The relative pressures and its relative errors in the function of the volume porosity

The closes result has been achieved with 0.363 volume porosity, when the relative error was lower than 2.5%. Of course, closer results could be achieved with more simulations, but this accuracy is satisfying from our viewpoint.

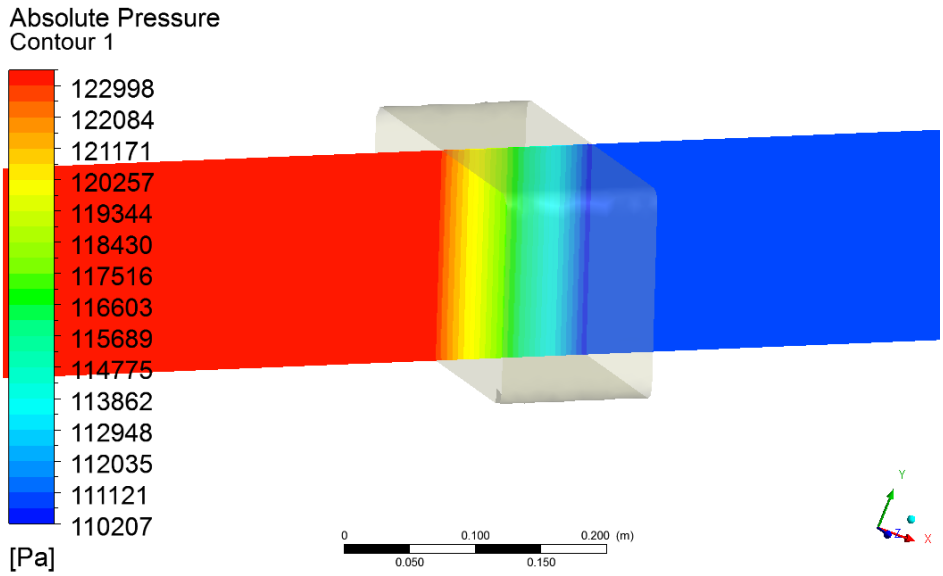

Figure 8. Absolute pressure difference distribution in the longitudinal cross section of the model; the pressure drop is highlighted in the middle, porous section

As Figure 7 shows, the absolute pressure, which is set to the inlet boundary of the geometry, is constant till the inlet surface of the porous domain. Because of the isotropic loss model, then the pressure starts to decrease, till the end of the porous domain, downstream of that the pressure remains constant till the outlet of the fluid domain.

The volume porosity, the permeability and loss coefficients had to be checked whether the characteristics of the porous domain is similar to the experimental data. In order to be able to check the differences for every cases, given in Table 3 a simulation has been created. The settings were the same, only the inlet and outlet boundary conditions have been modified, and

because of the density dependence of the loss coefficient, K_{loss} has been calculated for each case independently. The listed settings are summarized in Table 5.

Cooling air mass flow [kg/s]	Inlet relative pressure [Pa]	K_{loss} [1/m]
0,1511975	11358,45	173,4183
0,3023949	13301,35	170,4789
0,4535924	15244,24	167,6375
0,6047898	17934,40	163,856
0,7559873	21521,28	159,0717
0,7937866	22119,10	158,3014
0,9071847	25407,07	154,1944
1,0583822	29890,67	148,9256
1,2095797	35420,44	142,9033

Table 5. The recalculated boundary conditions of the checking simulation cases

With similarly computational demands and run time (every case has converged in 50 iteration steps) the results have been examined in the same way: the absolute pressure has been surface-averaged in the inlet and outlet boundary of the porous domain. In the function of the simulated velocity and the mass flow, which latter was a boundary condition, but is the best comparison to the original experimental data, the pressure drop values (pressure difference between the inlet and outlet absolute pressure) have been plotted (see in Figure 9 and Figure 10).

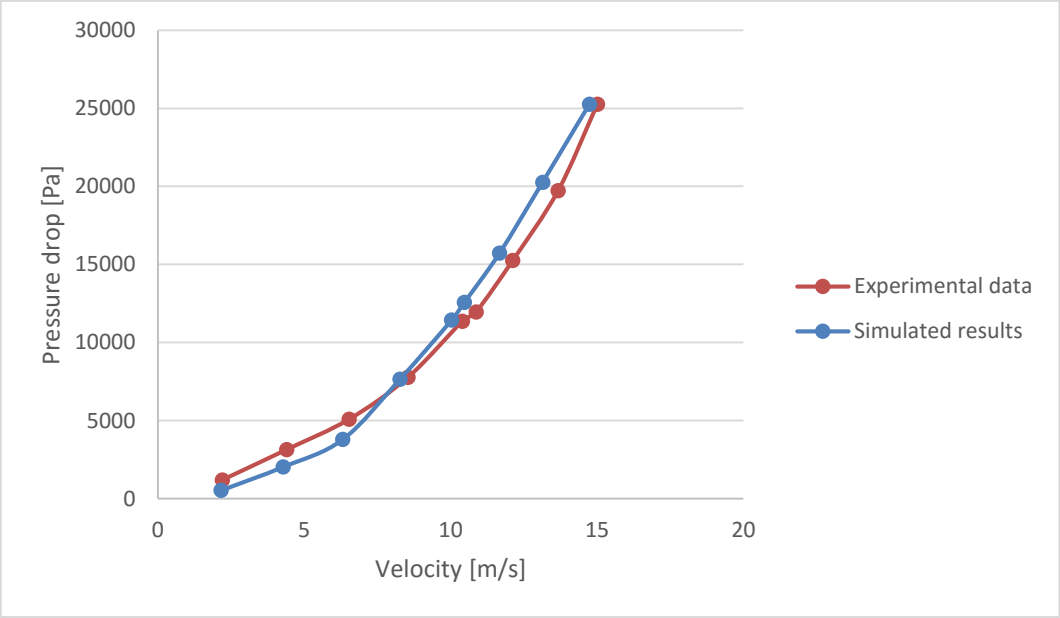

Figure 9. The pressure drop in the function of the inlet velocities at the porous domain inlet

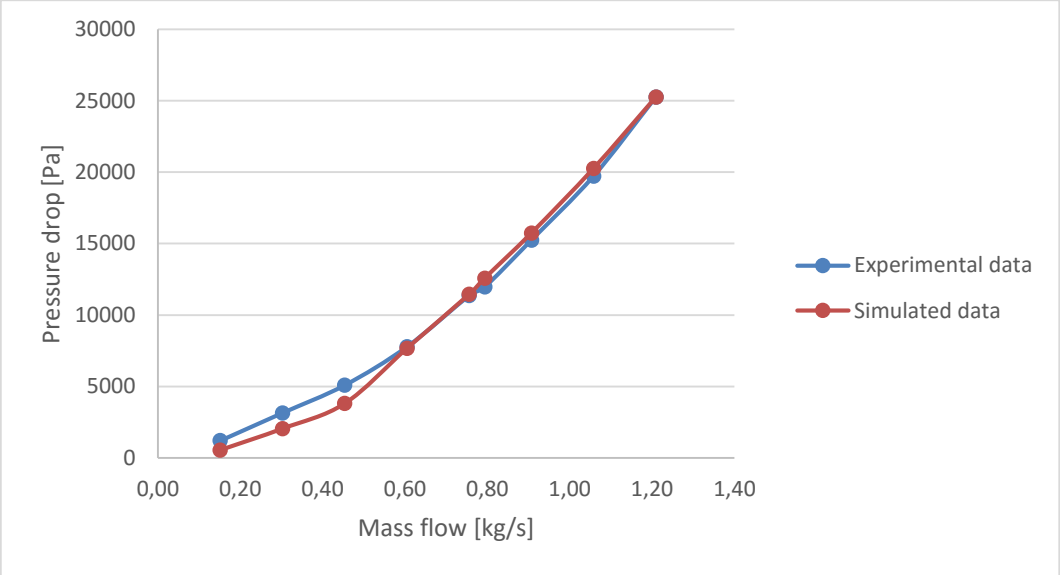

Figure 10. The pressure drop values in the function of the mass flow

As the two diagrams show: minor differences can be seen, but the relative error, referred to the related inlet pressure values, is 0.458%. The errors could be minimized by fining the iteration process, or by get more accurate experimental results. A small misreading can cause non-negligible differences in the final results, but the efficiency of the method itself is independent from the input data; more accurate inputs provide more accurate output.

Basically we can state that the investigation was successful; with the manually calculated porous domain settings, and the volume porosity determination with iterating simulations have provided a method, which is capable to handle the air flow conditions inside a heat exchanger without creating the detailed mesh inside the device, which would increase the computational time significantly.

CONCLUSIONS

The scope of the paper is to introduce a simple method, which is capable to simulate the wading effect of an oil-to-air, plate-fin type heat exchanger to the cooling airflow (cold side), and can be integrated into more complex simulations. The project has been done in the framework of the ESPOSA project, where the BME Department of Aeronautics, Naval Architecture and Railway Vehicles participates, and investigates the airflow around a small aircraft turboprop, engine nacelle, and inside the air intake duct and an oil-to-air heat exchanger. The configuration consists the plate-fin type heat exchanger, which had to be examined, what kind of effect it has to the external airflow, so a simple method was required, which computational demands are not high. By researching in the literature, it was found, that the porous media is capable to handle this function. In the Theoretical Fundamentals chapter the governing equations have been introduced, just like the most important equations, which describe the behaviour of the porous media.

The simulation, is introduced in this paper, focuses on the heat exchanger, so the main boundaries of the device have been kept, and all other parts, like ducts, fins, plates etc. have been deleted. The heat exchanger basically has been replaced by a cuboid with rounded edges; there

is the porous domain. Upstream and downstream of the porous domain the cuboid has been extracted to 5 times of the original depth of the porous domain, and two fluid domains have been created. For the discretization method tetra elements have been used, though the model is perfect for applying hexa type elements, the complex simulation, for which this simulation has been developed, is built up with tetra elements. Thus, if we want to receive similar results, same mesh pattern had to be applied. The size of the mesh was fitted to the overall mesh sizes, so every surface and volume elements were set to 10 mm. On the walls boundary layers have been applied; with 8 mm height 8 inflation layers were inserted with 1.5 prism ratio. Finally 1204103 elements and 294923 nodes have been created.

From the manufacturer provided data (pressure drop values for different mass flows), the characteristics of the heat exchanger has been determined: at first the cooling air mass flow and pressure drop values have been converted into SI dimensions, then the inlet pressure values have been calculated, from which the densities, and finally the inlet velocities have been determined. The inlet velocities were necessary, because for Darcy's law, the velocity – pressure drop function has to be determined. The calculated velocities have been checked with simulations, the difference between the calculated and computed velocities were smaller than 0.2 m/s in every cases. The velocity − pressure drop diagram has been created, and a parabolic trend curve has been inserted on the points, which crosses the "y" curve at 0. The quadratic and linear coefficients determine the K_{loss} and K_{perm} values, the final task is to determine the volume porosity (γ). In order to get this value, numerous simulations have been run with the same boundary conditions, but with different volume porosity setting. For the boundary conditions the sample case have been used, which was provided by the partner institute.

The generated pressure drop has been examined between the inlet and outlet surface of the porous domain, and when the results got close to the demand, the volume porosity value has been accepted. In our simulation the volume porosity as 0.363, where the computed pressure difference differed with absolute 2.3% compared to the target pressure drop value. To verify the model for the full range of the investigation, a simulation has been prepared for each cases, from which the parameters have been determined. The boundary condition settings were the same, except the inlet static pressure and mass flow values, which have determined the case, and except K_{loss}, which is influenced by the density, so this coefficient had to be calculated for each simulation case also. The results showed the same pattern as the experimental data; for the full range of the investigation the relative error, referred to the related inlet pressure values, is 0.458%.

Finally, it can be concluded, that if we consider only the pressure decreasing effect of a heat exchanger, without the heat transfer (from the viewpoint of the external airflow), the porous domain is capable to replace the heat exchanger with the calculation method and settings, which are described in this paper. The advantage of this assumption, that the computational demands are significantly lower, than if the air flow conditions inside the heat exchanger are simulated in details, but can give accurate results. Because of the low computational requirements, this solution can be useful especially in the pre-design and pre-sizing process of a small aircraft.

REFERENCES

[1] A. Berg: Numerical and experimental study of the fluid flow in porous medium in charging process of stratified thermal storage tank; M.S.c. Thesis; KTH School of Industrial Engineering and Management; Energy Technology EGI-2013-028MSC; Division of Applied Thermodynamics and Refrigeration, 2013

[2] A.C. Menon, S.A. Kumar: Experimental Study of Heat Transfer Through Porous Media During The Application of Radial Heat Flux Condition; International Journal of Emerging Technology and Advanced Engineering; ISSN 2250-2459, ISO 9001:2008 Certified Journal, Volume 3, Issue 10, October 2013

[3] A. Fakheri: Efficiency analysis of heat exchangers and heat exchanger networks; International Journal of Heat and Mass Transfer 76 (2014) 99–104; http://dx.doi.org/10.1016/j.ijheatmasstransfer.2014.04.027

[4] A. Gandhi, N. Asija, K.K. Gaur, S.J.A. Rizvi, V. Tiwari, N. Bhatnagar: Ultrasound assisted cyclic solid-state foaming for fabricating ultra-low density porous acrylonitrile–butadiene–styrene foams; Material Letters, Volume 94, 1 March 2013, Pages 76-78; doi:10.1016/j.matlet.2012.12.024

[5] A.K. Tiwari, P. Ghosh, J. Sarkar: Heat transfer and pressure drop characteristics of CeO2/water nanofluid in plate heat exchanger; Applied Thermal Engineering 57 (2013) 24-32; http://dx.doi.org/10.1016/j.applthermaleng.2013.03.047

[6] A. Neale, D. Derome, B. Blocken, J. Carmeliet: Coupled Simulation of Vapor Flow between Air and a Porous Material; Thermal Performance of the Exterior Envelopes of Whole Buildings X International Conference Proceedings, December 1-5, 2007

[7] Ansys, Introduction to CFX, Chapter 3: Domains and Boundary Conditions, presentation http://wenku.baidu.com/view/86c366a1284ac850ad024201.html?re=view

[8] Ansys CFX-Solver Theory Guide; Release 12.0; April 2009

[9] A. Szymkiewicz: Modelling Water Flow in Unsaturated Porous Media; 2013, XXII, 238 p., Hardcover, ISBN:978-3-642-23558-0

[10] B. Gáti, A. Drouin: Open Source Autopilot for Academic Research – The Paparazzi System, Proceedings of the American Control Conference, Washington DC: AACC International, pp. 1-6. ISBN: 978-1-4799-0175-3, 2013.

[11] B. Parikshit, K.R. Spandana, V. Krishna, T.R. Seetharam, K.N. Seetharamu: A simple method to calculate shell side fluid pressure drop in a shell and tube exchanger; International Journal of Heat and Mass Transfer 84 (2015) 700–712; http://dx.doi.org/10.1016/j.ijheatmasstransfer.2015.01.068

[12] C.-C. Cheng, S.-M. Tsai, H.-P. Cheng, C.-H. Chen: Analysis for heat transfer enhancement of helical and electrical heating tube exchangers in vacuum freeze-drying plant; International Communications in Heat and Mass Transfer 58 (2014) 111–117, http://dx.doi.org/10.1016/j.icheatmasstransfer.2014.08.032

[13] C.-C. Wang, K.Y. Chen, J.-S. Liaw, C.-Y. Tseng: An experimental study of the air-side performance of fin-and-tube heat exchangers having plain, louver, and semi-dimple vortex generator configuration; International Journal of Heat and Mass Transfer 80 (2015) 281–287; http://dx.doi.org/10.1016/j.ijheatmasstransfer.2014.09.030

[14] C. Haslego, A. Laval, G. Polley: Designing Plate-and-Frame Heat Exchanger; www.pinchtechnology.com; September 2002; Compact Heat Exchangers Part 1

[15] D.A. Nield, A. Bejan: Convection in Porous Media; 2nd ed. 1999, XXI, ISBN 978-1-4757-3033-3

[16] D. Rohács: Potential European Small Aircraft Prediction and Demand Models; Proceedings of the 6th International Conference on Nonlinear Problems in Aviation and Aerospace (ICNPAA), Budapest, Hungary, June 21-23, 2006. pp605-616

[17] D. Taler, P. Ocłoń: Determination of heat transfer formulas for gas flow in fin-and-tube heat exchanger with oval tubes using CFD simulations; Chemical Engineering and Processing 83 (2014) 1–11; http://dx.doi.org/10.1016/j.cep.2014.06.011

[18] D. Taler, P. Ocłoń: Thermal contact resistance in plate fin-and-tube heat exchangers, determined by experimental data and CFD simulations, International Journal of Thermal Sciences 84 (2014) 309-322; http://dx.doi.org/10.1016/j.ijthermalsci.2014.06.001

[19] D. Youchison, J. Garde, B. Williams, M. Wright: Heat Transfer in High-Temperature Refractory Foam Heat Exchangers; PFC meeting presentation, DL Youchison 134012/02

[20] http://www.engineeringtoolbox.com/dry-air-properties-d_973.html

[21] ESPOSA Integrated Project – Level 2, Aeronautics and Air Transport; BE2 TR2 WP6.4 Requirements; prepared by EVEKTOR; 1st October 2011, GRANT AGREEMENT NO. ACP1-GA-2011-284859-ESPOSA

[22] G.A. Quadir, I.A. Badrudding, N.J. Salman Ahmed: Numerical Investigation of the performance of a triple concentric pipe heat exchanger; International Journal of Heat and Mass Transfer 75 (2014) 165–172;

[23] H.-J. Steeman, A. Janssens, M. De Paepe: Coupling moisture transport in air flows and porous materials using CFD; 8th Nordic Symposium on Building Physics 2008
[24] H.N.G. Wadley, D.T. Queheillalt: Thermal Applications of Cellular Lattice Structures; Materials Science Forum Vols. 539-543 (2007) pp. 242-247
[25] HydrocarbonEngineering Journal: The Pressure Drop; February 2009; http://www.tranter.com/literature/products/The%20pressure%20drop%20HCE%20Feb%202009.pdf
[26] J. Fernández-Sear, R. Diz, F.J. Uhía: Pressure drop and heat transfer characteristics of a titanium brazed plate-fin heat exchanger with offset strip fins; Applied Thermal Engineering 51 (2013) 502-511; http://dx.doi.org/10.1016/j.applthermaleng.2012.08.066
[27] J.M. Yin, C.W. Bullard, P.S. Hrnjak: Pressure Drop Measurements in Microchannel Heat Exchanger; ACRC CR-30; April 2000
[28] J. Rohács: Evaluation of the air transport efficiency definitions and their impact on the European personal air transportation system development, Transactions of the Institute of Aviation, Scientific Quarterly 3/2010 (205), "EPATS European Personal Air Transportation Systems - selected issues, Institute of Aviation, Warsaw, 2010, pp 14 - 32, ISSN 0509-6669
[29] K. Beneda J. Rohács: Dynamic Model of Variable Inducer Shroud Bleed for Centrifugal Compressor Surge Suppression, International Review of Aerospace Engineering 6: (3) pp. 163-173. Paper online, 2013.
[30] K. Beneda: CFD Simulation of Blade Load Distribution Control as Active Centrifugal Compressor Surge Suppression, ACTA AVIONICA 15:(25) pp. 13-20. 201
[31] K. Boomsma, D. Poulikakos, F. Zwick: Metal foams as compact high performance heat exchangers; Mechanics of Materials 35 (2003) 1161–1176
[32] K. Krishnakumar, A.R. Nair: Determination of heat transfer and flow friction of a porous body using modified slope method; Proceedings of the 37th International & 4th National Conference on Fluid Mechanics and Fluid Power; December 16-18, 2010, IIT Madras, Chennai, India; FMFP10 – HT – 24
[33] M.A. Biot: General Solutions of the Equations of Elasticity and Consolidation for a Porous Material; Journal of Applied Mechanics, March 1956
[34] M.A. Delavar, M. Azimi: Using Porous Material for Heat Transfer Enhancement in Heat Exchangers: Review; Journal of Engineering Science and Technology Review 6 (1) (2013) 14-16; ISSN: 1791-2377
[35] M. Goyal, A. Chakravarty, M.S. Atrey: Two dimensional multistream plate fin heat exchangers; Cryogenics 61 (2014) 70-78; http://dx.doi.org/10.1016/j.cryogenics.2014.02.017
[36] M.H. Panjeshahi, Nassim Tahouni: Pressure drop optimization in debottlenecking of heat exchanger networks; Energy 33 (2008) 942–951; doi:10.1016/j.energy.2007.09.013
[37] M.K. Aliabadi, M.G. Samani, F. Hormozi, A.H. Asl: 3D-CFD Simulation and neural network model for the j and f factors of the wavy fin-and-flat tube heat exchangers; Vol. 28, No. 03, pp. 505 - 520, July - September, 2011; ISSN 0104-6632
[38] M. Khoshvaght-Aliabadi, F. Hormozi, A. Zamzamian: Role of channel shape on performance of plate-fin heat exchangers: Experimental assessment, International Journal of Thermal Sciences 79 (2014) 183-193; http://dx.doi.org/10.1016/j.ijthermalsci.2014.01.004
[39] M. Khoshvaght-Aliabadi, S. Zangouei, F. Hormozi: Performance of a plate-fin heat exchanger with vortex-generator channels: 3D-CFD simulation and experimental validation; International Journal of Thermal Sciences 88 (2015) 180-192; http://dx.doi.org/10.1016/j.ijthermalsci.2014.10.001
[40] M.O. Adebajo, R.L. Frost, J.T. Kloprogge, O. Carmody, S. Kokot: Porous Materials for Oil Spill Cleanup: A Review of Synthesis and Absorbing Properties; Journal of Porous Materials 10: 159-170, 2003
[41] M.S. Peters, K. Timmerhaus, R.E. West: Heat-Transfer Equipment – Design and Costs; Plant Design and Economics for Chemical Engineers, 5/e
[42] P. Forooghi, K. Hooman: Experimental analysis of heat transfer of supercritical fluids in plate heat exchangers; International Journal of Heat and Mass Transfer 74 (2014) 448–459; http://dx.doi.org/10.1016/j.ijheatmasstransfer.2014.03.052
[43] P. Pongsoi, S. Pikulkajorn, S. Wongwises: Heat transfer and flow characteristics of spiral fin-and-tube heat exchangers: A review; International Journal of Heat and Mass Transfer 79 (2014) 417–431; http://dx.doi.org/10.1016/j.ijheatmasstransfer.2014.07.072
[44] R.C. Tew, T. Simon, D. Gedeon, M.Ibrahim, W. Rong: An Initial Non-Equilibrium Porous-Media Model for CFD Simulation of Stirling Regenerators; NASA/TM – 2006-214391

[45] R. Nebbali, A. Bousri: Forced Convection Heat Transfer Enhancement Using Porous Blocks within Channels; Proceedings of the International Conference on New Trends in Transport Phenomena; Ottawa, Ontario, Canada, May 1-2 2014; Paper No. 45
[46] S.B. Saad, P. Clément, J.-F. Fourmigué, C. Gentric, J.-P. Leclerc: Single phase pressure drop and two-phase distribution in an offset strip fin compact heat exchanger; Applied Thermal Engineering 49 (2012) 99-105; doi:10.1016/j.applthermaleng.2011.09.022
[47] Seventh Framework Programme, Theme [AAT.2011.4.4-4.], Project ESPOSA: Annex I – "Description of Work"; Grant agreement no: 284859; Version date: 2011-09-20
[48] S.P. Kearney, A.M. Jacobi: Local and Average Heat Transfer and Pressure Drop Characteristics of Annularly Finned Tube Heat Exchangers; ACRC Project TR-69, January 1995
[49] S. Sharafat, A. Mills, D. Youchison, R. Nygren, B. Williams, N. Ghoniem: Ultra low pressure-drop helium-cooled porous-tungsten PFC; Fusion Science and Technology Vol. 52. October 2007
[50] S. Soltani, S. Shafiei: Heat exchanger retrofit with considering pressure drop by coupling genetic algorithm with LP (linear programming) and ILP (integer linear programming) methods; Energy 36 (2011) 2381e2391; doi:10.1016/j.energy.2011.01.017
[51] T.Gao, B. Sammakia, J. Geer: Dynamic response and control analysis of cross flow heat exchangers under variable temperature and flow rate conditions; International Journal of Heat and Mass Transfer 81 (2015) 542–553; http://dx.doi.org/10.1016/j.ijheatmasstransfer.2014.10.046
[52] V. Kumar, D. Gangascharyulu, P.M.S. Rao, R.S. Barve: CFD analysis of cross flow air to air tube type heat exchanger; http://www.cham.co.uk/puc/puc_melbourne/papers/paper18_kumar.pdf
[53] X.X. Zhu, X.R. Nie: Pressure drop consideration for heat exchanger network grassroots design; Computers and Chemical Engineering 26 (2002) 1661/1676; PII: S 0098 - 1354(02)00149-7 http://dx.doi.org/10.1016/j.ijheatmasstransfer.2014.03.042
[54] Y. Yang, Y. Li: General Prediction of the thermal hydraulic performance for plate-fin heat exchanger with offset strip fins; International Journal of Heat and Mass Transfer 78 (2014) 860–870; http://dx.doi.org/10.1016/j.ijheatmasstransfer.2014.07.060
[55] Y. Zhou, L. Zhu, J. Yu, Y. Li: Optimization of plate-fin heat exchangers by minimizing specific entropy generation rate; International Journal of Heat and Mass Transfer 78 (2014) 942–946; http://dx.doi.org/10.1016/j.ijheatmasstransfer.2014.07.053
[56] http://wenku.baidu.com/view/86c366a1284ac850ad024201.html?re=view
[57] W. Xuehong, Z. Wenhui, G. Qiuping, L. Zhiming, L. Yanli: Numerical simulation of heat transfer and fluid flow characteristics of composite fin; International Journal of Heat and Mass Transfer 75 (2014) 414–424; http://dx.doi.org/10.1016/j.ijheatmasstransfer.2014.03.087
[58] W.Yaïci, M. Ghorab, E. Entchev: 3D CFD analysis of the effect of inlet air flow maldistribution on the fluid flow and heat transfer performances of plate-fin-and-tube laminar heat exchangers; International Journal of Heat and Mass Transfer 74 (2014) 490–500; http://dx.doi.org/10.1016/j.ijheatmasstransfer.2014.03.034
[59] W. Yao, X. Chen, W. Luo, M. van Tooren, J. Guo: Review of uncertainty-based multidisciplinary design optimization methods for aerospace vehicles; Progress in Aerospace Sciences, 42 (2011) 450-479, doi:10.1016/j.paerosci.2011.05.001
[60] Z. Čarija, B. Franković, M. Perčić, M. Čavrak: Heat transfer analysis of fin-and-tube heat exchangers with flat and louvered fin geometries; International Journal of Refrigeration 45 (2014) 160-167; http://dx.doi.org/10.1016/j.ijrefrig.2014.05.026